

## Chapter 2

### Fundamental Theory

#### 2.1 The Physics of Star Formation

If molecular clouds are condition sites of star formation, what the must exist for collapse to occur? Sir James Jeans first investigated this problem in 1902 by considering the effects of a small deviation from hydrostatic equilibrium within a cloud. Although several assumptions were made in the analysis, such as neglecting the effects of rotation and galactic magnetic fields, it provided important insights into the development of protostars.

##### 2.1.1 Hydrostatic Equilibrium

For a cloud to be stable against collapse or expansion, the internal pressure must exactly balance gravity at all positions within the cloud. This is called *hydrostatic equilibrium*. The conditions for hydrostatic equilibrium can be derived as follows:

Consider a small volume in a static spherical gas cloud of mass  $M$  and uniform density  $\rho$  (Figure 2.1).

The inward gravitational force ( $F_{in}$ ), on the disk of cross-section area,  $A$ , and height,  $dr$ , is given by

$$F_{in} = -m_d \frac{GM_r}{r^2} \quad (2.1)$$

where  $M_r$  is the total mass within the radius  $r$ , and  $m_d = A\Delta r\rho$  is the mass of the disk.

The outward force,  $F_{out}$ , is simply the internal gas pressure, which is given by

$$F_{out} = A\Delta P \quad (2.2)$$

where  $\Delta P$  is the force per unit area on the surface of the disk.

For equilibrium,

$$F_{out} = F_{in}, \quad (2.3)$$

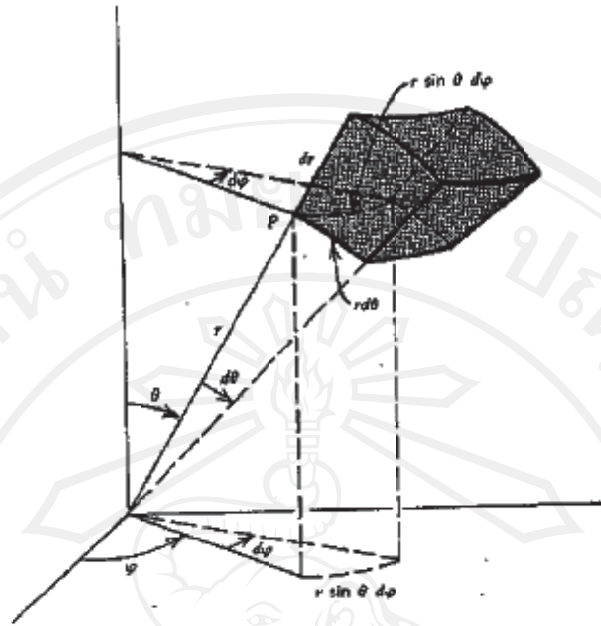


Figure 2.1: Model spherical gas cloud of mass  $M$  and uniform density  $\rho$

from which one obtains

$$A\Delta P = -A\Delta r\rho\frac{GM_r}{r^2} \quad (2.4)$$

which can be written

$$\frac{dP}{dr} = -\frac{GM_r\rho}{r^2} = -g_r\rho \quad (2.5)$$

where the acceleration caused by gravity at a position,  $r$ , must be  $g_r = \frac{GM_r}{r^2}$ .

The pressure gradient is balanced by gravity at all points for hydrostatic equilibrium.

Consider a system with a large number of particles, such as a molecular cloud, with a fluid density,  $\rho$ . For a sphere of constant density,  $\rho$ , the mass  $M$  and radius  $R$  are

related by

$$M = \frac{4\pi}{3}R^3\rho$$

The gravitational potential energy,  $U$ , is equivalent to the work required to bring all the mass  $M$  from infinity to the final radius  $R$ .

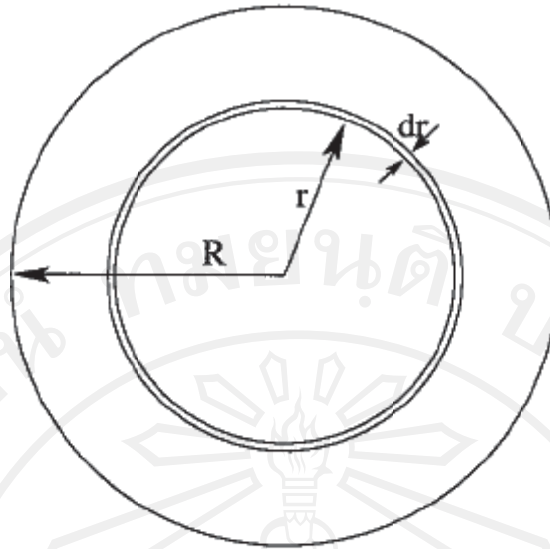


Figure 2.2: Volume Model

Consider a thin shell of thickness  $dr$  at radius  $r$  (Figure 2.2)

The volume of this thin shell is;

$$dV = 4\pi r^2 dr \quad (2.6)$$

and its mass,  $dM$ , is;

$$dM = 4\pi r^2 dr \rho. \quad (2.7)$$

The total mass,  $M$ , within the radius  $r$  is;

$$M = \frac{4\pi}{3} r^3 \rho \quad (2.8)$$

The gravitational potential energy,  $U$ , between any two points is given by

$$U = -\frac{Gm_1m_2}{r} \quad (2.9)$$

From this, it can be shown that the potential energy of a sphere of radius,  $R$ , and mass,  $M$ , is (Asanok, 2006)

$$U = -\frac{3GM^2}{5R} \quad (2.10)$$

From this it can be shown that the kinetic energy is

$$K = \frac{3}{2}NkT = \frac{3M}{2\mu}kT \quad (2.11)$$

where  $N$  is the total number of particles in the cloud and  $\mu$  is the mean mass per particle ( $N = M/\mu$ ).

### 2.1.2 Collapsing Clouds

From the virial theorem,

$$-2K = U \quad (2.12)$$

if twice the total internal kinetic energy of a molecular cloud ( $2K$ ) is greater than the absolute value of the gravitational potential energy ( $|U|$ ), then the gas pressure force will dominate over the gravitational force and the cloud will expand. If the internal kinetic energy is smaller, then the cloud will collapse. From the virial theorem, the condition for collapse ( $|U| \geq 2K$ ) becomes

$$\left| \frac{3GM^2}{5R} \right| \geq 3kT \frac{M}{\mu} \quad (2.13)$$

which implies that

$$\frac{M}{R} \geq \frac{5kT}{G\mu} \quad (2.14)$$

The mass  $M$  and the radius  $R$  are not independent variables since they are related to the density by the relation

$$\rho = \frac{M}{(4\pi/3)R^3} \quad (2.15)$$

Assuming that the density of the cloud,  $\rho$ , is constant over the whole cloud,

$$R = \left( \frac{3M}{4\pi\rho} \right)^{1/3} \quad (2.16)$$

Let us now try to estimate the size of the smallest cloud of a given density  $\rho$ , mean mass per particle  $\mu$  and temperature  $T$  which can collapse. From the above equations and in an idealized case

$$\frac{M}{R_j} = \frac{5kT}{G\mu} \quad (2.17)$$

or

$$\frac{4\pi R_j^3 \rho}{3R_j} = \frac{5kT}{G\mu} \quad (2.18)$$

where  $R_j$  is the **Jeans Radius** or the radius at which the thermal energy and the gravitational potential are equal.

Solving for  $R_j$ :

$$R_j = \left[ \frac{15kT}{4\pi\mu\rho G} \right]^{1/2} \quad (2.19)$$

It is often convenient to express the  $M/R$  relation in term of the *minimum mass* or *Jean Mass*,  $M_j$ , for which a cloud of density,  $\rho$ , mean particle mass,  $\mu$ , and temperature,  $T$ , will be just gravitationally stable. This can be done as follows:

$$M_j = \frac{4\pi R_j^3 \rho}{3} \quad (2.20)$$

$$= \frac{4\pi}{3} \left[ \frac{15kT}{4\pi\mu\rho G} \right]^{3/2} \rho \quad (2.21)$$

$$= \left[ \frac{5kT}{\mu G} \right]^{3/2} \left[ \frac{3}{4\pi\rho} \right]^{1/2} \quad (2.22)$$

which can be written in terms of the gas density  $n = \frac{\rho}{\mu}$

$$M_j \approx \left[ \frac{5kT}{\mu G} \right]^{3/2} \left[ \frac{3}{4\pi\mu n} \right]^{1/2} \quad (2.23)$$

Once a cloud becomes gravitationally bound, it will begin to collapse. We now want to estimate how long it will take to collapse to a stellar size if unimpeded by other forces.

The acceleration of a particle at radius  $r$  is given by :-

$$\begin{aligned} a(r) &= \frac{GM_r}{r^2} \\ &= \frac{4\pi}{3} r \rho G \end{aligned}$$

or

$$\frac{1}{r} \frac{d^2 r}{dt^2} = \frac{4\pi}{3} r \rho G$$

Solving this equation of motion for a time which we will call  $t_{ff}$ , **The Free-Fall Time**, give

$$t_{ff} = \left( \frac{3\pi}{32G\rho_0} \right)^{1/2} \quad (2.24)$$

where  $\rho_0$  is the initial density. The free-fall time depends only on the density and not cloud mass.

If the initial cloud out of which a star formed has any small amount of net angular momentum, as any real cloud will surely have (e.g. galactic rotational shear and other bulk motions), then this will be conserved as collapse proceeds. The angular momentum is given by

$$L = I\omega \quad (2.25)$$

where  $I$  is the moment of inertia and  $\omega$  is the angular speed of the cloud. For a sphere of radius,  $r$ , it can be shown that

$$I = \frac{2}{5}Mr^2, \omega \propto \frac{1}{r^2}$$

If  $I_0$  and  $\omega_0$  are initial values, then  $I_0\omega_0 = I\omega$  at any other time from the conservation of  $L$ . From this, it can be inferred that

$$\frac{\omega}{\omega_0} = \left(\frac{r_0}{r}\right)^2 \quad (2.26)$$

In the case of cloud collapse, the radial acceleration of a test particle of mass  $m$  at radius  $r$  will have two components

1. gravity:  $a_g(r) = GM(r)/r^2$  which is directed *radially towards the centre*
2. a centripetal term  $a_c(r) = r\omega^2$  directed *away from the axis of rotation*. The radial component of  $a_c(r)$  is

$$a_c(r) = r\omega^2 \sin\phi \quad (2.27)$$

where  $\phi$  is the angle from the axis of rotation to the particle as seen from the centre. (Figure 2.3)

Thus the net radial acceleration is:

$$a(r) = a_g(r) + a_c(r) = \frac{GM(r)}{r^2} - r\omega^2 \sin\phi \quad (2.28)$$

This shows that  $a(r)$  is smaller for a rotating cloud than for a non-rotating cloud. Further, at the pole ( $\phi = 0$ ),  $a(r) = g(r)$ , but at the equator ( $\phi = 90$ )

$$a(r) = g(r) - r\omega^2 \quad (2.29)$$

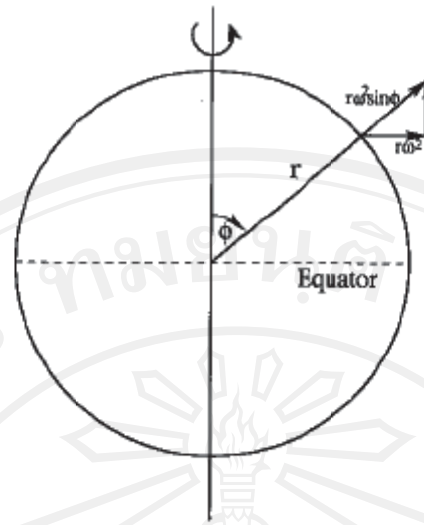


Figure 2.3: Show angle  $\phi$  from the axis to the particle as seen from the center

Now let's look at the dependence on  $r$  of  $a_g$  and  $a_c$  for matter in the equatorial plane where both components of acceleration are radial. Assuming that the mass written to our contracting mass point is constant, then  $a_g \propto \frac{1}{r^2}$  and  $a_c \propto r\omega^2 \propto \frac{1}{r^3}$  since  $\omega \propto \frac{1}{r^3}$ . By how much does the cloud contract before  $a_c = a_g$ , i.e.

$$\frac{GM(r)}{r^2} = r\omega^2 \quad (2.30)$$

which gives,

$$GM(r) = r^3\omega^2 \quad (2.31)$$

since  $\omega = \omega_0(r_0/r)^2$  then

$$GM(r) = r^3\omega_0^2(r_0/r)^4 \quad (2.32)$$

$$= \omega_0^2 \frac{r_0^3}{r} \quad (2.33)$$

and writing  $v_0 = \omega_0 r_0$  then

$$GM(r) = \frac{v_0^2 r_0^2}{r} \quad (2.34)$$

where  $v_0$  is an orbital velocity.

As collapse proceeds, an initially large, massive cloud will flatten around the equatorial plane. However, matter in the equatorial disk (accretion disk) can contract

only so far until it is stopped by rotation, at which point the cloud is likely to fragment into smaller pieces of higher density. These fragments can then contract further until they reach their orbital motion at which point further fragmentation takes place and so on. This process probably until fragments of about a Jeans mass and radius are formed, at which point the process of star formation can take place. This is why most stars are formed as part of a star cluster rather than as individual isolated stars.

## 2.2 Maser Theory

Masers, as their name implies, are the result of microwave amplification by stimulation emission of radiation. They arise naturally in space when the interstellar molecules are forced to interact with systems at several different temperatures and are unable to achieve a Maxwell-Boltzmann distribution of energies. The following sections introduce some of the main physical processes by Cohen (1989) and Elitzur (1992)

### 2.2.1 radiative transfer

The brightness or intensity of a radiation is defined as the energy per second per unit bandwidth per unit solid angle crossing unit area in the normal direction  $\hat{n}$ .  $I_\nu$  is measured in units of  $W m^{-2} Hz^{-1} sr^{-1}$  or in terms of brightness temperature (K) of an equivalent blackbody. Defining the specific emissivity,  $\epsilon_\nu$ , as the energy emitted per second per unit bandwidth per volume of the medium into unit solid angle. Thus the energy emitted into a cone of solid angle in time  $dt$  is given by

$$dE = \epsilon_\nu dV d\Omega d\nu dt \quad (2.35)$$

Defining the absorption coefficient  $\kappa_\nu$  as the fractional intensity absorbed from an incident beam per unit distance transmitted, then

$$dI_\nu = -\kappa_\nu I_\nu dS \quad (2.36)$$

For a beam of intensity  $I_\nu$  and solid angle  $d\Omega$  passing through a cylinder of length  $dS$  and cross section  $dA$ , the energy is

$$dE = \kappa_\nu I_\nu dA dS d\Omega d\nu dt \quad (2.37)$$

The interaction between radio waves and the gas in the interstellar medium is governed by the equation of radiative transfer

$$\frac{dI_\nu}{dS} = -\kappa_\nu I_\nu + \epsilon_\nu \quad (2.38)$$

where  $I_\nu$  is the specific intensity of radiation,  $\epsilon_\nu$  is the emissivity and  $\kappa_\nu$  is the absorption coefficient of the gas. Consider for simplicity a two-level system. In the case the emissivity is

$$\epsilon_\nu = n_2 A_{21} \frac{h\nu_{21}}{4\pi} f(\nu) \quad (2.39)$$

where  $n_2$  is the number density in the upper level,  $A_{21}$  is the Einstein coefficient giving the probability of spontaneous emission,  $\nu_{21}$  is the mean frequency of the emitted photons and  $f(\nu)$  is the normalized line profile and  $h$  is the Planck constant. The absorption coefficient is

$$\kappa_\nu = n_1 B_{12} - n_2 B_{21} \frac{h\nu_{21}}{c} f(\nu) \quad (2.40)$$

where  $B_{21}$  is the Einstein coefficient for absorption and  $B_{12}$  is the coefficient for stimulated emission. The Einstein coefficients are related by the equations

$$A_{21} = B_{21} \frac{8h\nu^3}{\pi c^3} \quad (2.41)$$

and

$$B_{12} = \frac{g_2}{g_1} B_{21} \quad (2.42)$$

where  $g_i$  are the statistical weights of the upper and lower states.

The effect of stimulated emission is to reduce the absorption coefficient  $\kappa_\nu$ . These are usually specified by an *excited temperature*  $T_{ex}$  the temperature at which the populations would be in the Boltzmann ratio

$$\frac{n_2}{n_1} = \frac{g_2}{g_1} (-h\nu_{21}/kT_{ex}) \quad (2.43)$$

At ratio frequencies  $h\nu_{21}/k$  is of order 0.1 K, so for gas in local thermodynamic equilibrium the factor  $h\nu_{21}/kT_{ex}$  is very small and stimulated emission almost cancels absorption. The net absorption coefficient is thus the difference between two much larger terms which are almost equal. As a result the radiative transfer through the gas is very sensitive to small changes in the level population shifts.

The solution to the equation to transfer is readily found to be

$$I_\nu = I_\nu(0)\exp(-\tau_\nu) + \int_0^{\tau_0} \frac{j_\nu}{\kappa_\nu} \exp[-(\tau_\nu - \tau'_\nu)] d\tau'_\nu \quad (2.44)$$

where  $I_\nu(0)$  is the intensity of radiation entering gas and  $\tau_\nu$  is the optical depth defined by  $d\tau_\nu = \kappa_\nu dS$ . Normally the optical depth would be a positive number, and the radiation reaching the observer would be the background radiation  $I_\nu(0)$  attenuated by the factor  $\exp(-\tau_\nu)$ , plus the emission (and absorption) from the cloud itself. For a maser, the absorption coefficient is negative, the optical depth is negative and so is the excitation temperature.

### 2.2.2 Saturation

The radiation from cosmic masers usually grows to become so intense that the stimulated emission begins to reduce the population inversion. It is then said to saturate or only regions of the maser cloud are saturated.

The phenomenon of saturation has been treated by Goldreich & Keeley (1972) for two simple cases: uniform spherical masers and cylindrical masers. Their calculations are purely classical in which the level populations of a two-states maser are governed by the rate equations

$$\frac{dn_2}{dt} = -n_2 A_{21} - (n_2 - n_1) B_{21} J + P_2 (n - n_1 - n_2) - \Gamma_2 n_2 \quad (2.45)$$

and

$$\frac{dn_1}{dt} = n_2 A_{21} + (n_2 - n_1) B_{21} J + P_1 (n - n_1 - n_2) - \Gamma_1 n_1 \quad (2.46)$$

where  $n$  is the total density of the maser species,  $P_i$  is pump rate into level  $i$  from all levels other than 1 and 2.  $\Gamma_i$  is the loss rate from level  $i$  and

$$J = \frac{1}{4\pi} \iint I_\nu d\nu d\Omega \quad (2.47)$$

is the number of maser photons crossing unit volume per second. It has been assumed, without loss generality, that the statistical weights of the maser states are equal. For steady state

$$(n_2 - n_1)(2B_{21}J + \Gamma_2 + 2n_2A_{21}) = (P_2 - P_1(n - n_1 - n_2) + n_1(\Gamma_1 - \Gamma_2)) \quad (2.48)$$

The maser saturates wherever

$$J \sim \frac{\Gamma_2}{2B_{21}} = \frac{\Gamma_2}{A_{21}} \frac{4\pi\nu^3}{\pi c^3} \quad (2.49)$$

The solutions of the rate equations are then substituted into the equation of radiative transfer, which is effectively one dimensional for the cases considered by Goldreich & Keeley (1972).

### 2.2.3 Pumping Mechanism

The system particles tend to populate the ground state. They are excited into higher levels by either collisions or radiation from an external source. The pumping scheme is called *collisional* or *radiative* according to the nature of the process that dominates these excitations. The radiation produced internally in decays of excited states (the diffuse radiation) can never be considered the pumping agent: in the absence of external radiation or collision, all the system particles would cascade to the ground state and the diffuse radiation would disappear. But the diffuse radiation must always be taken into considerations because it can play an important role in shaping the population distribution among the system levels.

### 2.2.4 OH Maser Transitions

The first astronomical maser is also the first molecule detected in interstellar space at radio frequencies - OH, the hydroxyl radical. This molecule has been unfilled electron

shell and various internal spins. As a result, its energy level structure is fairly complex. Because the molecule is symmetric around the inter-nuclei axis, projections of internal angular momenta on this axis, chosen the z-axis, are conserved quantities. The overall angular momentum excluding nuclear spin is  $\mathbf{J} = \mathbf{K} + \mathbf{L} + \mathbf{S}$ , where  $\mathbf{K}$  corresponds to the molecular end-over-end rotation (so  $K_z = 0$ ),  $\mathbf{L}$  is the electronic angular momentum and  $\mathbf{S}$  is the electron spin ( $S = 1/2$ ). The ground electron state is a  $\Pi$ -state, with  $L_z = 1$ . Therefore  $J_z = 1 \pm 1/2$ , giving rise to two rotation ladders,  ${}^2\Pi_{1/2}$  and  ${}^2\Pi_{3/2}$ ; subscripts denote the value of  $J_z$  while the superscript 2 is used to denote the two possible electronic spin orientations. States on each ladder are characterized by their  $J$  ( $\geq J_z$ ). Interaction with the next electron configuration, a  $\Sigma$ -state, removes the degeneracy between states with  $+J_z$  and  $-J_z$ , introducing a parity splitting known as  $\Lambda$ -*doubling*. Further splitting is caused by hyperfine interaction with the nuclear spin  $\mathbf{I}$  ( $I = 1/2$ ). Each rotation state is thus split into four levels according to parity and  $F$  ( $= J \pm 1/2$ ), the value of the total angular momentum  $\mathbf{F} = \mathbf{J} + \mathbf{I}$ .

A comprehensive tabulation of relevant frequencies and A-coefficients was prepared by Destombes et al. (1977). An energy level diagram is shown in figure 2.4, displaying the rotation levels that couple radiatively to the ground state. Splitting within each rotation level is exaggerated for clarity. The scale on the right corresponds to wavelengths for transitions to the ground state, whose levels are plotted on an expanded scale at the right corner with transition frequencies (in MHz) marked on the arrows. OH allowed transitions follow the simple diode selection rules, which require a parity change and  $\Delta F = 0, \pm 1$  but  $F = 0 \rightarrow 0$  is forbidden). The wavelengths of the ground-state transitions are approximately 18 cm. The  $F$ -conserving lines, with frequencies of 1665 and 1667 MHz, are called *main lines* and the  $F$ -changing ones, at 1612 and 1720 MHz, are *satellite lines*. Maser emission has been discovered in all four ground state transitions, as well as in radio lines of low lying excited rotation states.

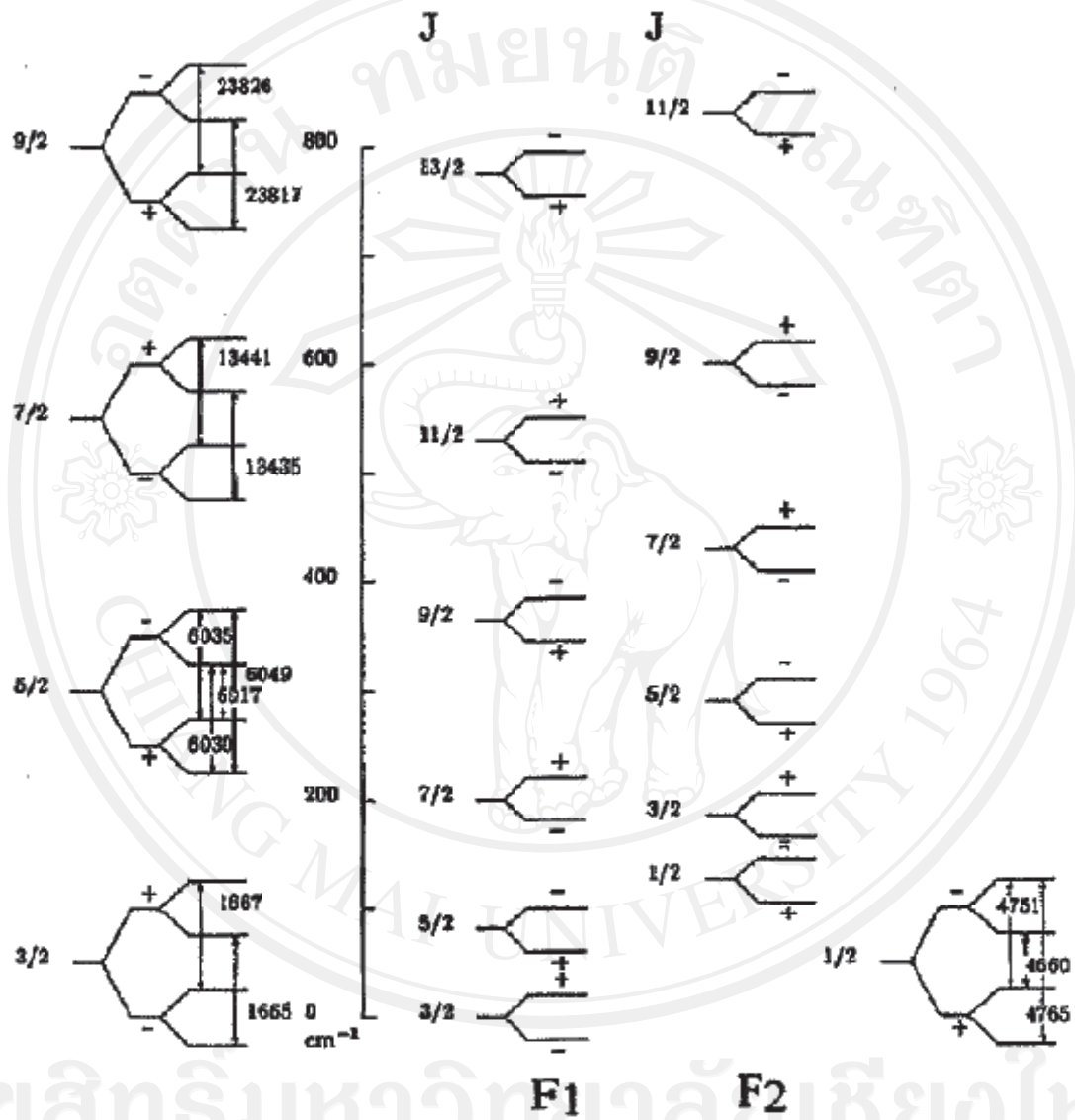


Figure 2.4: The rotational energy levels of OH showing  $\Lambda$ -doubling and nuclear hyperfine splitting.  $F_1$  and  $F_2$  corresponding to  ${}^2\Pi_{3/2}$  and  ${}^2\Pi_{1/2}$  respectively.

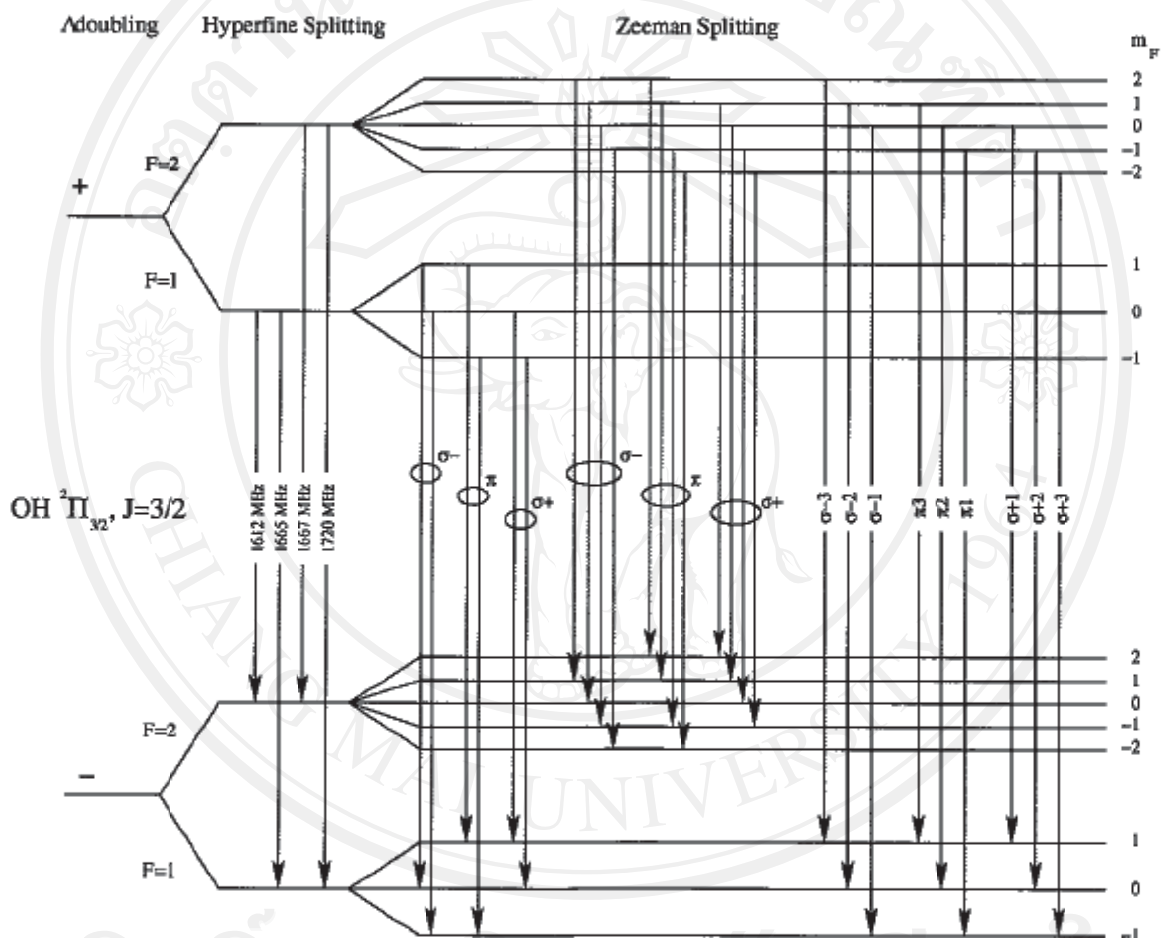


Figure 2.5: The energy levels of OH molecule in the ground state. In the magnetic field, there are four hyperfine transitions at 1612, 1665, 1667 and 1720 MHz.

## 2.3 Effect of magnetic field

### 2.3.1 The spin of the electron

The doublet energy levels could be classified by a new quantum number  $j$  with the two values

$$j = l + \frac{1}{2} \text{ and } j = l - \frac{1}{2} \quad (2.50)$$

for the upper and lower levels of the doublet, respectively. This new quantum number gives the magnitude of the total angular momentum  $J$  of the atom, according to the formula

$$|J| = j(j + 1) \quad (2.51)$$

The energy levels of most other atoms, with more than one electron, can be identified by a similar set quantum numbers. The net orbital angular momentum of the electrons in such an atom is the summation of the individual angular momentum of the electrons,

$$\mathbf{L} = \sum_i \mathbf{L}_i \quad (2.52)$$

Similarly, the net spin is

$$\mathbf{S} = \sum_i \mathbf{s}_i \quad (2.53)$$

and the total angular momentum is

$$\mathbf{J} = \mathbf{L} + \mathbf{S} = \sum_i \mathbf{L}_i + \sum_i \mathbf{s}_i \quad (2.54)$$

All of these angular momenta obey the usual quantization rules. Thus

$$|\mathbf{L}| = \sqrt{\mathbf{L}(\mathbf{L} + 1)\hbar} \quad (2.55)$$

$$|\mathbf{S}| = \sqrt{\mathbf{S}(\mathbf{S} + 1)\hbar} \quad (2.56)$$

$$|\mathbf{J}| = \sqrt{\mathbf{J}(\mathbf{J} + 1)\hbar} \quad (2.57)$$

### 2.3.2 The Zeeman Effect

The net magnetic moment of an atom is the vector summation of all the magnetic moments associated with the spin plus all the magnetic moments associated with the orbital motion. Using the Bohr model, we can understand how the orbital motion of an electron generates a magnetic moment. The magnetic moment is

$$\mu = -\frac{e}{2m_e} L \quad (2.58)$$

where  $L = m_e v r$  is the orbital angular momentum of the electron. Taking into account that the direction of the magnetic moment is related by the right-hand rule to the direction of the electric current. We can express as a vector equation as follows:

$$\mu_L = -\frac{e}{2m_e} L \quad (2.59)$$

$$\mu = -\frac{e}{2m_e} L - \frac{e}{2m_e} S = -\frac{e}{2m_e} (L + 2S) \quad (2.60)$$

To find the magnitude of net magnetic moment ( $|\mu|$ ) and the component  $\mu_z$  along the  $z$ -axis, we need to take into account the angular orientation of  $L$  and  $S$ . We will merely state the final result for  $\mu_z$ ,

$$\mu_z = -g m_J \frac{e\hbar}{2m_e} \quad (2.61)$$

where  $m_J = J, J-1, \dots, 1-J, -J$  and the factor  $g$ , the **Lande g-factor**, is

$$g = 1 + \frac{J(J+1) + S(S+1) - L(L+1)}{2J(J+1)} \quad (2.62)$$

Here the quantum number  $L$ ,  $S$  and  $J$  are related in the usual way to the magnitudes of the net orbital angular momentum, the net spin angular momentum, and the total angular momentum.

If we apply an atom in an external magnetic field, the interaction between the atomic magnetic moment and the magnetic field will shift and split the energy levels of the atom. The fine structure generates by the internal magnetic field of atom, we now get an extra structure generated by the external magnetic field acting on the atom. The splitting of spectral lines by external magnetic field is called the **Zeeman effect**. Since

it depend on the quantum numbers of the energy levels, it is very useful tool in the identification of these quantum numbers. The Zeeman effect is also very useful tool in astronomy because it permits the detection of the magnetic fields an stars, star-forming regions, and on the sun.

We can calculate the energy shift of an energy level in a magnetic field from an equation similar to Eq.(1). We assume that the magnetic field lies along the z-axis, Then

$$U = -\boldsymbol{\mu} \cdot \mathbf{B} = -\mu_z B \quad (2.63)$$

$$U = g m_J \frac{e \hbar B}{2 m_e} \quad (2.64)$$

This energy shift removes the degeneracy of states with different values of  $m_J$ : the states with different values of  $m_J$  have different energies by the effect of magnetic field.

The complicated splitting Zeeman effect is sometimes called the **anomalous Zeeman effect**. If the external magnetic field is very strong, in the order of 10 or more tesla, then the splitting becomes simple; it is called the **normal Zeeman effect**.

### 2.3.3 Zeeman Splitting in the OH Molecules

The  $\Pi$  ground electron states mentioned above in split into two state by  $\Gamma$  doubling, and these are doubled by hyperfine splitting, resulting in four states for each value of  $J$ . In a magnetic field, each of these states is further split into  $2F + 1$  magnetic energy sublevels separated from the original energy level by

$$\begin{aligned} \Delta W = h \Delta \nu = & - \mu_n g_I \cdot \frac{m_F B}{2F(F+1)} [I(I+1) + F(F+1) - J(J+1)], \\ & - \mu_0 g_J \cdot \frac{m_F B}{2F(F+1)} [J(J+1) + F(F+1) - I(I+1)] \end{aligned}$$

Where  $\mu_n$  and  $\mu_0$  are the nuclear and Bohr magnetron ( $\mu_n = \mu_0/1836$ )

$g_I \sim g_J \sim 1$  are the Lande g-factor;

$$\mu_0/h = 1.39967 \text{ MHz G}^{-1};$$

$J$  = quantum number for the angular momentum including rotation but excluding nuclear spin;

$F$  = total angular momentum;

$I$  = nuclear spin;

$m_F$  = the magnetic quantum number giving the projection of an direction of the magnetic field; it takes the values  $F, F - 1, \dots, -F + 1 - F$ ;

$B$  = the magnetic field strength.

The first term (interaction of the nuclear magnetic moment with the magnetic field) of splitting is negligible compared with the second term (the interaction of the electron magnetic moment with the magnetic field).

The Zeeman splitting pattern anticipated for a particular OH emission line results from transitions between the magnetic sublevels of the two states, the upper state ( $m_2$ ) and the lower state ( $m_1$ ). For the selection rules, the transitions allowed are  $\Delta m_F = m_2 - m_1 = -1, 0$  and  $+1$ . The  $\Delta m_F = 0$  transitions are called  $\pi$  components and the  $\Delta m_F = \pm 1$  transitions are called  $\sigma$  components. If no magnetic fields, the magnetic sub-levels are degenerate and all different  $m_2 \rightarrow m_1$  transitions occur at the common unperturbed frequency  $\nu_{21}$ . The magnetic sublevels, and the frequency become

$$g = g_J \frac{F(F+1) + J(J+1) - I(I+1)}{2F(F+1)} \quad (2.65)$$

and  $\Delta g = g_2 - g_1$ . For the  ${}^2\Pi_{3/2}$  state,  $J = 3/2, I = 1/2$  and the factor  $g_J$  is 0.935. When  $\Delta g = 0$ , as in the case of OH main lines (at 1665 and 1667 MHz), the frequency shifts depend only on  $\Delta m_F$  and are independent of the specific values of the magnetic quantum numbers. Only three Zeeman components are generated in this cases, corresponding to  $\Delta m_F = 0, \pm 1$ . But in OH satellite lines (1613 and 1720 MHz), where  $\Delta g \neq 0$ , the frequency of each transition  $m_2 \rightarrow m_1$  is shifted by a different amount, which depends on both  $m_1$  and  $m_2$ , leading to nine Zeeman components. The resulting Zeeman patterns for the  ${}^2\Pi_{3/2}$  star are shown in figure 2.6

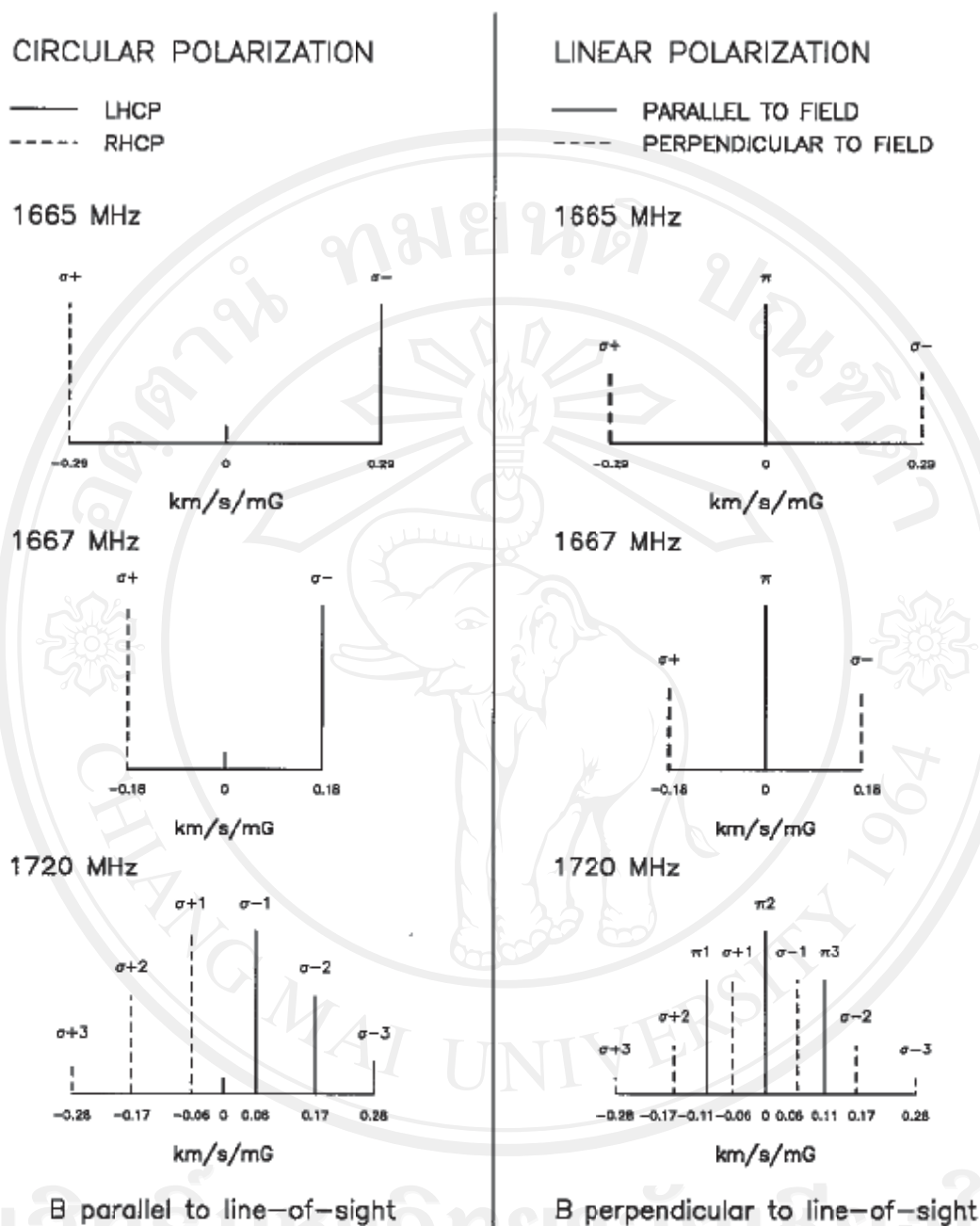


Figure 2.6: Zeeman splitting patterns for the  $^2\Pi_{3/2}$ ,  $J = 3/2$  state of OH molecule.

The splitting is plotted in units of velocity (km/sec/mG). Relative intensities of the Zeeman components are shown for each transitions from Davies (1974) and references therein. The patterns in left-hand side of the figure result from observation parallel to the magnetic field and the direction of the magnetic field is pointing towards to the observer. Those on right-hand side are from observations perpendicular to the field.

Table 2.1: Zeeman splitting of the  ${}^2\Pi_{3/2}$ ,  $J = 3/2$  ground state of OH molecule ( $\sigma$  components); see Davies (1974)

Transitions	Frequency (MHz)	Zeeman splitting between	Velocity Splitting ( $\text{km s}^{-1}\text{mG}^{-1}$ )
${}^2\Pi_{3/2}$ , $J = 3/2$ :			
$F = 1 \rightarrow 1$	1665.402	$\sigma^+ \leftrightarrow \sigma^-$	0.590
$F = 2 \rightarrow 2$	1667.359	$\sigma^+ \leftrightarrow \sigma^-$	0.354
$F = 2 \rightarrow 1$	1720.530	$\sigma^{+1} \leftrightarrow \sigma^{-1}$	0.114
		$\sigma^{+2} \leftrightarrow \sigma^{-2}$	0.342
		$\sigma^{+3} \leftrightarrow \sigma^{-3}$	0.570

## 2.4 Polarization

### 2.4.1 Wave Polarization

Consider a plane wave traveling out of the page (positive  $z$  direction), as in Figure 2.7(a) with the electric field at all times in the  $y$  direction. This wave is said to be *linearly polarization* (in  $y$  direction). As a function of time and position, the electric field is given by

$$E_y = E_2 \sin(\omega t - \beta z) \quad (2.66)$$

The electric field of a wave traveling in the  $z$  direction may have both a  $y$  component and a  $x$  component, as suggested in Figure 2.7(b) In this more general situation, with a phase difference  $\delta$  between the components, the wave is said to be *elliptically polarized*. At a fixed value of the  $z$ , the electric vector  $E$  rotates as a function of time, that tip of the vector describing an ellipse called the *polarization ellipse*. The ratio of the major to minor axes is called the *axial ratio* (AR). For the wave in Figure 2.7(b),  $AR = E_2/E_1$ . Two extreme cases of elliptical polarization corresponding to *circular polarization* as in Figure 2.7(c) and *linear polarization* as in Figure 2.7(a). For circular polarization  $E_1 = E_2$  and  $AR = 1$ , while the linear polarization  $E_1 = 0$   $AR = \infty$ .

In the most general cases of elliptical polarization, the elliptically polarized

wave may be have any orientation. The elliptically polarized wave may be have expressed in the terms of two linearly polarized components, one in the  $x$  direction and one in  $y$  direction. Thus, if the wave are traveling in the positive  $z$  direction (out of the page), the electric field components in the  $x$  and  $y$  direction are

$$E_x = E_1 \sin(\omega t - \beta z) \quad (2.67)$$

$$E_y = E_2 \sin(\omega t - \beta z + \delta) \quad (2.68)$$

where

$E_1$  = amplitude of wave linearly polarized in  $x$  direction

$E_2$  = amplitude of wave linearly polarized in  $y$  direction

$\delta$  = time pase angle by which  $E_y$  and  $E_x$  Combining (2.67) and (2.68) gives the total vector field  $\mathbf{E}$

$$\mathbf{E} = \hat{x}E_1 \sin(\omega t - \beta z) + \hat{y}E_2 \sin(\omega t - \beta z + \delta) \quad (2.69)$$

For  $z = 0$ ,  $E_x = E_1 \sim \omega t$  and  $E_y = E_2 \sin(\omega t + \delta)$ , then  $E_y$  yields

$$E_y = E_2(\sin\omega t \cos\delta + \cos\omega t \sin\delta) \quad (2.70)$$

If  $E_1 = 0$  the wave is linearly polarized in the  $y$  direction. If  $E_2 = 0$ , the wave is linearly polarized in  $x$  direction. If  $\delta = 0$  and  $E_1 = E_2$ , the wave is linearly polarized but in a plane at an angle of 45 degree with respect to the  $x$  axis. If  $E_1 = E_2$  and

$\delta = \pm 90^\circ$ , the wave is circularly polarized. When  $\delta = +90^\circ$ , the wave is *left circularly polarized*, and when  $\delta = -90^\circ$ , at  $z = 0$  and  $t = 0$ , that  $E_x = 0$  and  $\mathbf{E} = \hat{y}E_2$ . Under the same condition but  $\omega t = 90^\circ$ ,  $E_y = 0$  and  $\mathbf{E} = \hat{x}E_1$ . Thus, at a fixed position  $z = 0$  the electric vector rotates clockwise.

## 2.4.2 Faraday Rotation

Faraday rotation or Faraday effect is a rotating of the plane of polarization of the linearly polarized electromagnetic waves as they pass through a magnetic field in a plasma.

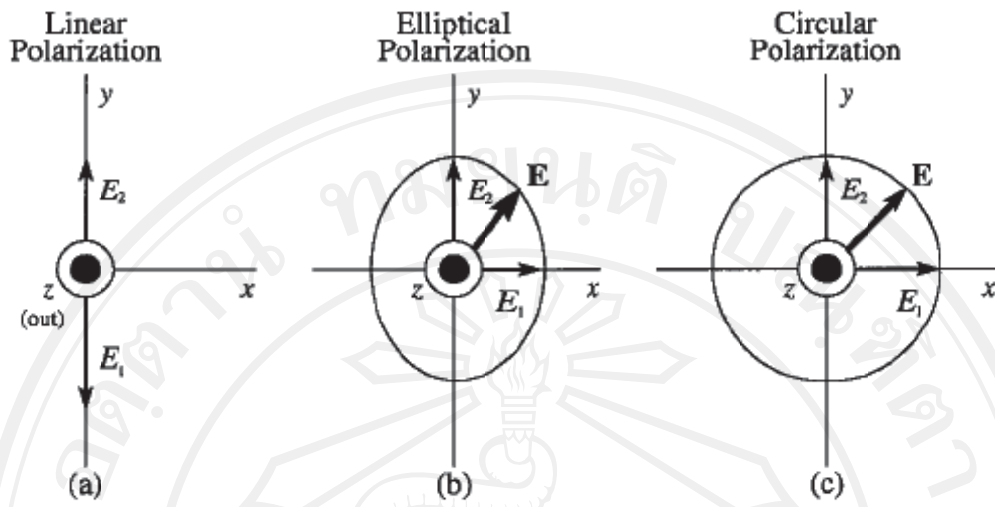


Figure 2.7: Relation of instantaneous electric field  $E$  to polarization ellipse

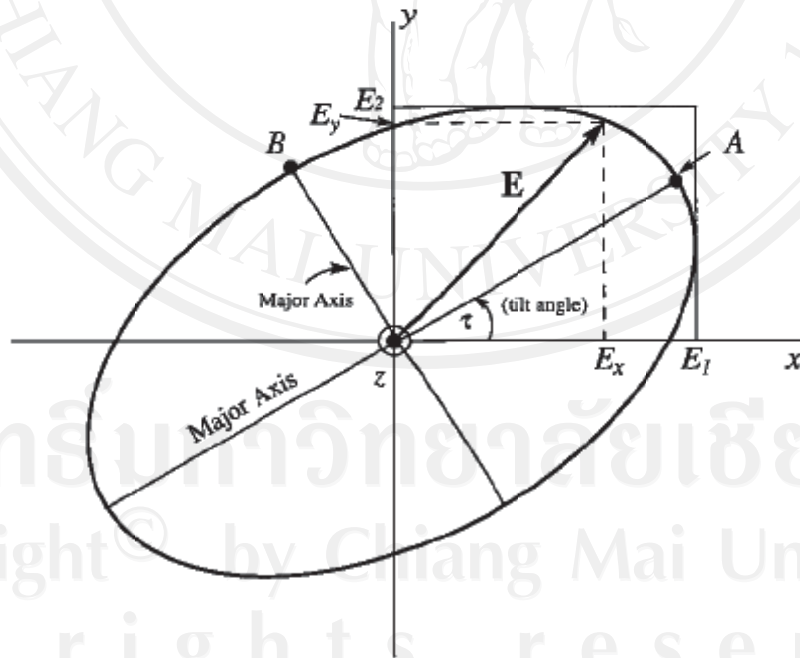
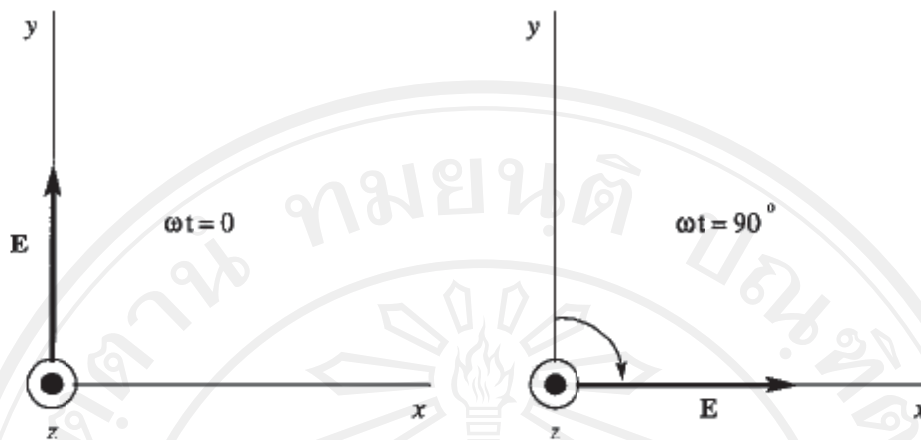


Figure 2.8: Polarization ellipse at tilt angle  $\tau$  showing instantaneous components  $E_x$  and  $E_y$  and amplitudes (or peak values)  $E_1$  and  $E_2$

Wave approaching

Figure 2.9: Change in direction of  $\mathbf{E}$  for left circular polarization

A linearly polarized wave may be thought of as the sum of two circularly polarized waves of opposite hand. That is, one wave is polarized to the right and one wave is polarized to the left (both waves are at the same frequency). When the linearly polarized wave passes through a magnetic field, the right-polarized wave component travels very slightly faster than the left-polarized wave component. The total *Faraday rotation* for the quasi-longitudinal case ( $\phi$  small) is then

$$\theta = \frac{e^3 \lambda^2}{8\pi^2 c^3 \epsilon_0 m^2} \int_0^r N B \cos \phi dr \quad (2.71)$$

where

$e$  = charge of particle, coulomb

$m$  = mass of particle, kg

$\epsilon_0$  = permittivity of free space, farad  $m^{-1}$

$c$  = velocity of light, m/s

$N$  = number of particles, number  $m^{-3}$

$B$  = magnetic flux density, weber  $m^{-2}$

$\phi$  = angle between  $\mathbf{B}$  and the direction of propagation

$r$  = distance in direction of propagation, m

If  $B$  and  $\phi$  are constant, becomes

$$\theta = \frac{e^3 \lambda^2}{8\pi^2 c^3 \epsilon_0 m^2} \int_0^r N dr \quad (2.72)$$



ลิขสิทธิ์มหาวิทยาลัยเชียงใหม่  
 Copyright© by Chiang Mai University  
 All rights reserved